Sawtooth pacing with on-axis ICRH modulation in JET-ILW

E. Lerche[1,2], M. Lennholm[1], I. S. Carvalho[1,3], P. Dumortier[1,2], F. Durodie[2], D. Van Eester[2], J. Graves[4], Ph. Jacquet[1], A. Murari[5] and JET contributors[*]

EUROfusion Consortium, JET, Culham Science Centre, Abingdon, OX14 3DB, UK

[1] *Euratom/CCFE Fusion Association, Culham Science Centre, Abingdon, United Kingdom*
[2] *LPP-ERM/KMS, Association EUROFUSION-Belgian State, TEC partner, Brussels, Belgium*
[3] *Instituto de Plasmas e Fusão Nuclear, Association EUROFUSION -IST, Lisbon, Portugal*
[4] *CRPP-EPFL, Association EUROFUSION - Confédération Suisse, Lausanne, Switzerland*
[5] *Consorzio RFX, Association EUROFUSION – CNR/ENEA, Padova, Italy*

Abstract. A novel technique for sawteeth control in tokamak plasmas using ion-cyclotron resonance heating (ICRH) has been developed in the JET-ILW tokamak. Unlike previous ICRH methods, that explored the destabilization of the internal kink mode when the radio-frequency (RF) wave absorption was placed near the q=1 surface, the technique presented here consists of stabilizing the sawteeth as fast as possible by applying the ICRH power centrally and subsequently induce a sawtooth crash by switching it off at the appropriate instant. The validation of this method in JET-ILW L-mode discharges, including preliminary tests in H-mode plasmas, is presented.

1. Introduction

In tokamaks, the central plasma parameters commonly exhibit a non-linear oscillation, known as the sawtooth instability. A necessary condition for the instability is that the plasma current is sufficiently large with respect to the toroidal magnetic field for the safety factor (q) in the plasma centre to be smaller than unity. The sawtooth cycle manifests itself through a slow increase in the plasma temperature (and other parameters) in the central part of the plasma, followed by an abrupt crash – the sawtooth crash, usually resetting the plasma profiles approximately to those at the start of the cycle. At the sawtooth crash, the temperature in the central part of the plasma falls abruptly, while the temperature in the external plasma regions increases. The minor radius, separating the central plasma region, where the temperature decreases at a crash, from the exterior plasma region, where the temperature increases, is known as the sawtooth inversion radius. The position of the inversion radius is seen to be closely associated with the q=1 flux surface, reflecting the fact that the sawtooth crash is initiated by the growth of an $(N,M) = (1,1)$ kink mode [1-3]. Sawteeth, which were first reported in [4], are themselves relatively benign, causing a moderate confinement degradation without affecting the overall plasma stability. Recently, their role in avoiding core accumulation of heavy impurities in high performance plasmas in metallic machines has also been envisaged. [5-6].

Large sawtooth crashes can, however, trigger more deleterious instabilities, such as neo-classical tearing modes (NTMs), associated with other flux surfaces where the safety factor q is a rational number (typically q=2 or q=3/2) [7-8]. Such NTMs will reduce the plasma confinement significantly and, if the instability grows sufficiently large, they are likely to lead

---

[*] See the *Appendix of F. Romanelli et al., Proc. of the 25th IAEA Fusion Energy Conference, 2014, St. Petersburg, Russia*

to a plasma disruption, where the plasma disappears in the matter of milliseconds potentially causing significant damage to the tokamak. Standard theoretical models of NTMs indicate that they are meta-stable and only grow when triggered by a perturbation in the magnetic topology – the most common cause being magnetic perturbations associated with sawtooth crashes [7-8]. Large sawtooth crashes following long quiescent periods without a crash have been seen to be much more likely to trigger NTMs than crashes associated with a shorter inter-crash interval. For this reason it is important to assure that the sawtooth period (τ_{SWT}) remains shorter than the threshold for NTM triggering. Nevertheless, it is important to point out that shortening the sawtooth period does result in a moderate confinement reduction and for this reason it is desirable to maintain as long a sawtooth period as possible without inducing NTMs. For optimal performance conditions, it is therefore advantageous to develop methods to control the sawtooth period to a pre-determined value for high performance plasma scenario development.

A number of different methods have been developed to control the sawtooth period. The traditional actuators which have proved effective in implementing such control are Electron Cyclotron Resonance Heating and Current Drive (ECRH) and Ion Cyclotron Resonance Heating and Current Drive (ICRH). ECRH can affect the sawtooth period by driving current near the q=1 surface, modifying the local current profile in this region. Experiments and modelling on the control of the sawtooth period using ECRH are reported in [8-19]. Two separate methods for controlling the sawtooth period can be considered. In continuous control schemes, the ECRH power is kept constant while the ECRH deposition location is controlled in real-time to achieve the desired sawtooth period. Such control has been demonstrated on Tore Supra [11-12] and TCV [13]. Alternatively the ECRH power can be modulated with a modulation period equal to the desired sawtooth period. Such modulation described as sawtooth pacing or sawtooth locking has been analysed in and experimentally demonstrated, first on TCV [16-17] and later on FTU [18]. In addition to affecting the local current profile near q=1, in the same way as ECRH, ICRH can also influence the sawtooth period by modifying the pressure and distribution function of energetic ions in the plasma. Initial assessments of this effect are described in [20-25]. In [25] the fast ions are described through a fast ion pressure profile allowing the calculation of criteria for the triggering of a sawtooth crash. More recent work [26] has shown the importance of details of the orbits of the fast ions circulating near the q=1 surface. Sawtooth control based on variation of the fast ion distribution function has been demonstrated on JET [4, 6, 27-32], including real time control of the deposition location through variation of the ICRH frequency [32]. It is likely that the fast ion orbit effect was also responsible for the sawtooth control reported in [33-34].

The current paper describes the first demonstration of sawtooth control through modulation of the ICRH power. The concept is similar to the ECRH pacing [16] and locking [17] experiments on TCV with the difference being that the main effect of the ICRH modulation is a change of the fast ion population rather than a modulation of the q-profile near the q=1 surface. Sawtooth pacing acting on the fast ion stabilization properties is inherently slower than pacing based on q-profile (local current-drive) perturbations since the slowing-down dynamics of the fast ions is part of the pacing process. The main advantage of the former technique is that it relies on central ICRH deposition rather than power deposition near q=1 and therefore the location of the ICRH power is not critical as long as a large fraction of the power is deposited within the q=1 surface. As a consequence the ICRH can be deposited at the optimal location required by other considerations, such as for avoiding central accumulation of heavy impurities in high performance experiments in metallic machines, such as in JET-ILW [35-42] and AUG [43-45]. A possible disadvantage of this method is the fact

that the de-stabilization trigger (induced by removing ICRH power from the plasma core) has to compete with other stabilization mechanisms present in the discharge, such as those related to neutral beam injection (NBI) injection and fusion born alpha-particles. The required strength of the ICRH perturbation necessary for successful sawtooth pacing relative to the background stabilizing mechanisms has still to be quantified. A more stringent mathematical analysis of the conditions required for efficient pacing of sawteeth and edge-localized modes (ELMs) are given in [46], while an assessment of the similarities of ELM and sawtooth control and the relative merits of pacing and continuous controllers are given in [47].

This paper is divided as follows. In section 2, a brief review of the sawtooth stabilisation criteria are given [11,48], showing the impact of the ICRH power absorption on the core discharge properties. In section 3, the results of efficient sawtooth control with pre-programmed ICRH modulation in JET-ILW L-mode plasmas are discussed while in section 4 a real time controlled modulation scheme, which maximises the ICRH duty-cycle while assuring that the sawtooth period stays below the required maximum for NTM avoidance, is described. In section 5, some preliminary results of sawtooth control in moderate power H-mode discharges (P_{NBI}=8-12MW) are presented. Section 6 discusses the correlation between the sawtooth triggering time and the slowing-down of the fast (ICRH-accelerated) ions in different conditions. The paper ends with a summary and suggestions for further developing this technique in high NBI power plasma scenarios, where competing sawtooth stabilization mechanisms become important.

2. Basic stability criterion

In this section we describe the main parameters which, according to our model, determine the sawtooth dynamics. This description illustrates how various external actuators influence the sawteeth. We will especially concentrate on the influence of ICRH power and how modulating this power allows the sawtooth period to be controlled.

A sawtooth crash occurs when a certain criteria is fulfilled. At the crash a number of plasma parameters, most importantly the current profile, are reset to an initial value. Subsequently the plasma profiles evolve slowly towards a final value. This evolution is interrupted by a new sawtooth crash when the crash criteria are fulfilled again. The sawtooth period is therefore determined by a combination of the crash criteria and the time constant for the inter crash evolution. The latter is dominated by current diffusion while the crash conditions are affected by a number of different parameters as described in [25] and [26]. The methods used to control the sawtooth period, described in [5-6, 9-19, 26-34, 46-48] and the method described in the current paper, all control the sawtooth period by affecting the parameters which determine the crash criteria, in particular the properties of the fast ions distribution function.

In the plasma conditions relevant for the current paper, the crash criteria described by [25] can be reduced as follows. A sawtooth crash will occur when both of the following conditions are fulfilled

(1) $s_1 = \left(\frac{r}{q} \frac{dq}{dr} \right)_{q=1} > s_{crit}$

(2) $\delta \hat{W} < c_\rho \hat{\rho}$

Here s_1 is the shear at the $q=1$ surface and s_{crit} is the critical shear which depends on the layer physics at the $q=1$ surface. $\delta\hat{W}$ is the normalised potential energy functional associated with the $M=1$ mode which is responsible for the sawtooth crash. $\hat{\rho}$ is the ion Larmor radius normalised to the minor radius of the $q=1$ surface (r_1) and c_ρ is a constant of the order of unity. The normalised potential energy functional can be split in two components: $\delta\hat{W} = \delta\hat{W}_0 + \delta\hat{W}_{fast}$ where $\delta\hat{W}_{fast}$ is associated with the fast ion population in the plasma. In the context of the sawtooth instability, the primary effect of ICRH is to modify the fast ion population. In ref. [25] $\delta\hat{W}_{fast}$ is given as being proportional to $\int_0^1 x^{3/2}\frac{dp_{fast}}{dx}dx$, where $x = r/r_1$, r is the minor radius and $p_{fast}(x)$ is the fast ion pressure profile. This is an approximation and [26] has shown that $\delta\hat{W}_{fast}$ depends strongly on the orbits of the fast ions in the vicinity of the $q=1$ surface. While the fast ion pressure profile dependence on $\delta\hat{W}_{fast}$ always gives positive values for $\delta\hat{W}_{fast}$ the orbit effect allows this functional to be negative as well as positive. This fact has been exploited in the experiments described in [27-32] to destabilise the $M=1$ and shorten the sawtooth period below the natural sawtooth period which is observed without the additional ICRH power. Following a sawtooth crash s_1 is reduced to a low value (0 if the Kadomtsev model for the sawtooth is considered). After a sawtooth crash s_1 increases as current diffuses towards the plasma centre. When $\delta\hat{W} < c_\rho\hat{\rho}$ a sawtooth crash will occur when $s_1 > s_{crit}$. If, on the other hand, $\delta\hat{W} > c_\rho\hat{\rho}$, no sawtooth crashes will occur even when $s_1 > s_{crit}$. One could suspect that this means that no sawtooth crashes will occur at all for large fast ion pressures. This is however not true, as $\delta\hat{W}$ decreases with increasing s_1, $\delta\hat{W} \propto \delta W / s_1$. Using this fact, equation (2) can be expressed as $s_1 > s_W$, where s_W depends on $\delta\hat{W}$ and $\hat{\rho}$. Using this formulation allows us to rewrite (1) and (2) as a single equation

$$(3) \quad s_1 > \max(s_{crit}, s_W)$$

In this equation s_W can be modified by inducing fast ions by ICRH power injection. In the case of central ICRH deposition, the orbits of the fast ions results in an increase in s_W. As central ICRH heating only has a very modest influence on s_{crit} and s_1, an increase of s_W significantly above s_{crit} is the only way the sawtooth lengthening observed in discharges with central ICRH power can be explained in terms of eq.(3). The sawtooth pacing mechanism discussed in this is based on using central ICRH power to induce longer sawteeth by increasing s_W beyond s_{crit} and then briefly switching this power off to reduce the fast ion content and thereby s_W. As s_W is dominant at the time of the switch-off, this will lead to a reduction in $\max(s_{crit}, s_W)$ and a sawtooth crash will be provoked when (3) is fulfilled.

Figure (1a) shows a sketch of how s_1 and a parameter representing the fast ions evolves during the sawtooth cycle under various conditions. The stabilising effect of fast ions is seen by the increasing value s_1 required to enter the unstable region as the fast ion population increases. If the fast ion population is too small to make s_W larger than s_{crit}, no sawtooth lengthening will result. This is represented by the horizontal lower boundary of the unstable

region. A sawtooth crash is triggered when the trajectory in s_1 - fast ion space enters the unstable region. In this sketch it is assumed that s_1 goes to zero and that the fast ion profile is flattened at a sawtooth crash. Three different trajectories are shown, one for the case where the ICRH power is too low to have any effect, one for the case with significant ICRH power and a high value of s_1 at the crash and one for the pacing case, where the ICRH is switched off during the current diffusion phase, rapidly reducing the fast ion content and inducing a sawtooth crash. Figure (1b) shows how this would look as a function of time. The model used to produce this graph is very simplistic and is only intended to illustrate the sawtooth pacing mechanism.

Between sawtooth crashes the temperature, current and fast ion profiles are assumed to follow simple first order evolutions towards final profiles with the evolutions given by

$$(4) \quad X(t,r) = \left(X_{final}(r) - X(t_0,r) \right)\left(1 - e^{\frac{-t+t_0}{\tau_X}} \right) + X(t_0,r)$$

Here $t = t_0$ is the time of a sawtooth crash and $X(t,r)$ represents temperature, current or fast ion profiles at time t with r being the minor radius. $X_{final}(r)$ represents the final profiles at $t = \infty$. These profiles are actually never reached as the evolution is interrupted by the sawtooth crash. Different time constants (τ_X) are used to model the evolutions of current, temperature and fast ions. These time constants are chosen to achieve a reasonable position of the q=1 surface at the time of the crash and a reasonable central temperature behaviour. The time constant associated with the fast ion evolution is chosen to be in the range of the fast ion slowing down time. Figure 1 indicates that it should be feasible to pace sawteeth using the proposed method. The following sections show a series of experiments where this method is explored experimentally.
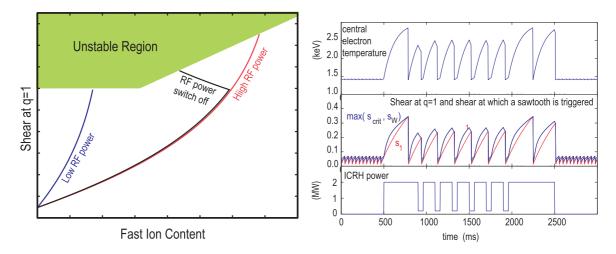

Figure 1: (a) Trajectories for the evolution between sawtooth crashes in (s_1 - fast ion content) space for different ICRH power levels. The knee in the black curve represents the moment where the ICRH power is switched off. A sawtooth crash will occur when the trajectories enter the unstable region and all parameters are reset to the initial values. (b) Simplistic simulation illustrating how trajectories from a) would appear as a function of time. No transport or current diffusion models are used. Profiles are assumed to follow a simple first order evolution towards final profiles. The fast ion evolution time constant is assumed to be similar to the fast ion slowing down time, while longer time constants are assumes for the temperature and current evolution. In this simulation the ICRH power is chosen to be sufficiently large for s_W to rise rapidly above s_{crit}. Under these conditions the notches in the RF power are seen to result in a reduction in $\max(s_{crit}, s_W)$ rapidly leading to a sawtooth crash.

3. L-mode results

The proof-of-principle of sawteeth control with on-axis ICRH modulation in JET-ILW was done in L-mode plasmas with B_0=2.7T / I_P=2MA, n_{e0}=(5±0.5)x10^{19}/m^3. Central hydrogen minority ICRH at f=42.5MHz (with dipole antenna phasing [49]) was used at the level of 3-4MW. Figure 2 shows the comparison between a discharge with constant ICRF power (left) and a discharge where the ICRH power was modulated at f_{mod}=5Hz with a duty-cycle of 75% (right). The non-modulated discharge is characterized by a sequence of long sawtooth build-ups followed by rapid crashes (b). The long sawteeth (with periods exceeding 0.5s) always trigger considerable magnet-hydro-dynamic (MHD) activity, though in this pulse do not causing lasting NTMs (c). It is interesting to note that, while this mode is present, the sawteeth are shorter and the plasma performance is degraded (d). When the ICRH power is modulated in otherwise identical plasma conditions, the sawteeth are efficiently paced at the RF modulation frequency and the N=2 MHD activity is fully suppressed. Despite the 25% lower averaged ICRF power applied, the peak temperatures are comparable to the constant ICRH power case. The total plasma stored energy is also similar in the two discharges, probably due to the absence of N=2 MHD activity in the modulated case which partially compensates for the 25% lower time averaged ICRH power applied (duty-cycle =75%). The insert in Fig.2b-right shows the details of the sawtooth pacing dynamics: The sawtooth crash is delayed with respect to the RF notch because it takes some time for the change in the fast particle population to impact the core electron profiles (slowing-down time).
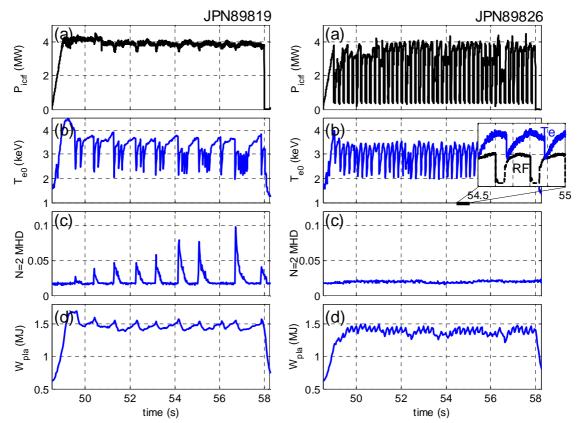

Figure 2: Comparison of two L-mode discharges with constant (89819) and 5Hz modulated (89826) ICRF heating, illustrating the successful sawtooth pacing and total suppression of the N=2 MHD activity in the latter: (a) ICRF power; (b) central electron temperature; (c) N=2 MHD mode amplitude; (d) plasma stored energy.

One of the main objectives of these exploratory experiments was to determine the range of modulation frequencies that can be used to reliably pace sawteeth. The main results are summarized in Fig.3, which shows the experimental sawtooth periods as function of (crash) time obtained in similar discharges with different RF modulation frequencies, $f_{mod} = 0$ (RF const.), 2Hz, 3Hz and 5Hz, all with duty-cycle=75%). The maximum RF power was roughly constant (P_{icrf}~4MW) and the H concentration was similar (X[H]=2-3%) in all discharges.

In the non-modulated case one recognizes the composite sawteeth dynamics with long (0.5-0.7s) sawteeth interleaved with very short ones. It is interesting to note that the sawtooth period remains short during phases with enhanced N=2 MHD activity (see Fig.2). This observation seems to hold true in a large number of discharges as also exemplified by the H-mode results presented in the next section (see Fig.6). This interesting observation deserves further experimental and theoretical investigation which is beyond the scope of the current paper. When the ICRF power is modulated at 2Hz, the maximum sawtooth period is, as expected, reduced to 0.5s but the shorter sawteeth still exist as long as the N=2 modes are not fully suppressed. In the 3Hz and 5Hz RF modulation cases, the N=2 activity is absent and the large majority of the sawteeth follow the RF modulation frequency, illustrating the efficient sawteeth control obtained in these conditions.

The relative number of RF-triggered sawteeth (normalized to the total number of sawteeth detected) increases with modulation frequency from 45% at 2Hz to 70% and 85% in the 3Hz and 5Hz cases, respectively, since less spontaneous sawteeth occur in the latter. Here, a sawtooth is considered as 'RF-triggered' if the sawtooth crash occurs within an interval of 20-80ms after an ICRH power notch (an interval consistent with the estimated min. and max. values of the slowing-down time of the fast ions). A more rigorous statistical analysis is given in section 6. The triggering efficiency, defined as the number of RF-triggered sawteeth divided by the number of RF notches is high in all cases, 80% at 2Hz, 83% at 3Hz and 88% at 5Hz, and does not depend strongly on the RF modulation frequency in the studied conditions.
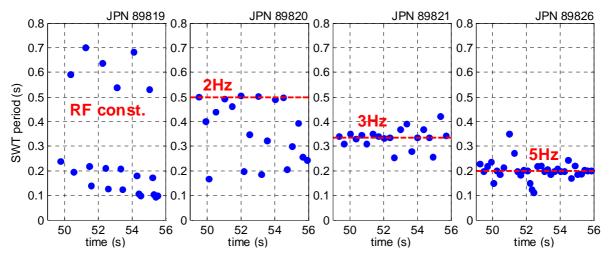

Figure 3: Sawtooth period vs. time for 4 similar L-mode discharges with constant and modulated ICRF power with fixed duty cycle = 75% (f_{mod} = 0, 2Hz, 3Hz, 5Hz).

The main drawback of imposing a prescribed RF modulation is that the ICRF power switch-off is not optimized, i.e. the power can be removed unnecessarily. Depending on the plasma properties or more specifically on the characteristic slowing-down time of the fast particles, this undesired effect occurs when natural sawteeth are faster than the RF modulation frequency as well as when the modulation is too slow altogether. Ways of minimizing these effects using real-time control of the RF modulation based on the measured sawteeth behaviour will be discussed in the next section.

4. Real time control

Despite the successful results, pre-programmed modulation waveforms have two disadvantages: (i) The power will be switched-off anyway, even if a sawtooth crash just occurred; (ii) The RF-off time interval is fixed, which reduces the effective (time averaged) ICRH power applied to the plasma. To minimize these undesired effects, a real-time control (RTC) of the RF power modulation was developed. The controller is based on real-time detection of the sawtooth crashes using an algorithm similar to the one described in [32] with the main difference being that a central soft X-ray channel was used rather than an ECE measurement. The working principle of the algorithm is simple: (i) Once a sawtooth is detected, the algorithm waits an imposed time interval (the assertion time Δt) before switching-off the ICRF power; (ii) As soon as it detects an RF-induced crash, it re-applies the ICRF power. A maximum time before the power is reapplied can also be set, in case the sawtooth detection fails.

An example of successful sawtooth pacing with real-time controlled RF modulation is given in Fig. 4, which shows the time traces of an L-mode discharge with similar parameters to the ones discussed in section 3. As requested, the ICRF power is removed $\Delta t =150$ms after the previous detected sawteeth crash, avoiding the occurrence of any long sawteeth (the natural sawtooth period is typically above 0.5s when the ICRF power is constant). The right figure (zoom) illustrates the main advantages of the RTC network: (i) The RF power is only removed after the assertion time of 150ms has elapsed since the last sawtooth crash (t=49.74s); (ii) The RF power is re-applied immediately after a sawtooth crash is detected (~6ms are necessary for sending the signal from the RTC network to the RF plant and reapply the power). Because the RF power is only switched-off when needed, the triggering efficiency is near 100% and the 'RF-off' time intervals (notches) are reduced with respect to the pre-programmed modulation cases.
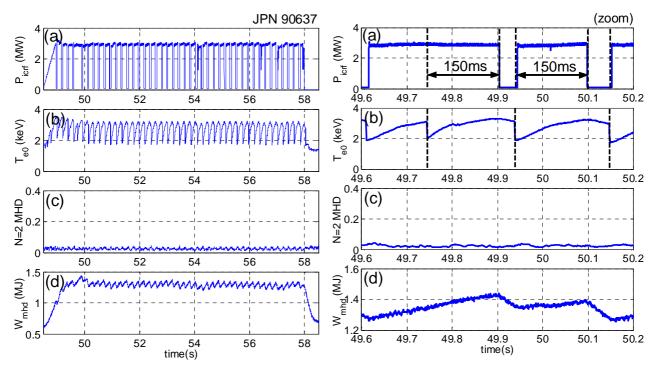

Figure 4: Example of an L-mode discharge with sawtooth pacing using real-time controlled ICRF modulation. The assertion time is 150ms leading to a constant sawtooth frequency of approximately 2Hz throughout the discharge.

Figure 5 shows the experimental sawtooth periods as function of (crash) time obtained in similar discharges with different real-time controlled ICRF modulation settings: $\Delta t= 2s$ (RF const.), 400ms and 150ms. The RF power ($P_{icrf}\sim3MW$) and the H concentration ($X[H]\sim3\%$) was similar in all discharges. The non-modulated (RF const.) discharge was performed with the RTC time delay set to a very large value (2s) so the power is never switched-off and the sawtooth dynamics is very similar to the reference discharge 89819 (Fig.2-left). The $\Delta t=400ms$ RT modulated case successfully limits the maximum period of the sawteeth to ~450ms, which corresponds to the switch-off time delay Δt added to the slowing-down time of the heated RF ions onto the electrons, as discussed later. Similar to pulse 89820 with fixed 2Hz RF modulation (Fig.3), shorter sawteeth still occur (interestingly concentrated around half the switch-off period) again coinciding with the presence of $N=2$ modes excited by large sawtooth crashes following longer (450ms) sawtooth intervals. The triggering efficiency is 100% but a large fraction of the sawteeth is shorter than the RF imposed period. The $\Delta t=150ms$ case shows 'perfect' sawtooth control at ~2Hz (consistent with Δt + slowing-down time) and the $N=2$ activity is completely absent. In this case the triggering efficiency is also 100% but practically all sawtooth crashes are induced by the ICRF notches.
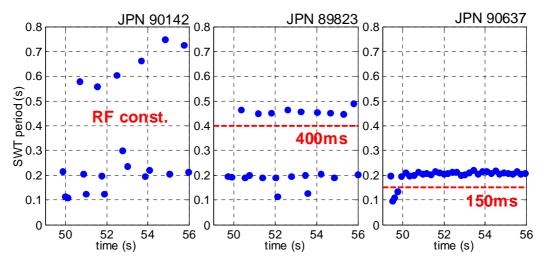

Figure 5: Sawtooth frequency vs. time for 3 similar L-mode discharges with different RTCC switch-off time delays: $\Delta t = 2s$ (RF const.), 400ms and 150ms. The actual sawtooth period expected corresponds to Δt + the electron slowing-down time of the fast ions (~2Hz and 5Hz).

The effective duty-cycle of the applied ICRH power in JPN 89823 (~2Hz modulation) was 95% (significantly higher than in the pre-programmed modulation discharges, 75-80%) reflecting the clear advantage of RT control to re-apply the RF power as quickly as possible. In JPN 90637 (~5Hz) the effective duty-cycle is reduced to 75%, since the RF-on period starts to become closer to the minimum necessary notch time for inducing a sawtooth crash (as discussed later). The natural reduction of the ICRH power duty-cycle with the sawtooth pacing frequency observed with real-time control of the RF modulation is not a problem in practice though, since the idea is to maximize the sawtooth period (higher T_{e0}) while still avoiding inducing deleterious MHD activity.

5. Preliminary H-mode results

In H-mode plasmas there are a few additional difficulties to be overcome for successful sawtooth control with ICRH: (i) The plasma density is higher and the RF-induced fast ion tails are harder to pull; (ii) The slowing-down time of the fast ions is typically longer and one could expect that larger RF notch times are needed to trigger a sawtooth crash; (iii) The central NBI ions also have a stabilizing influence on the internal kink mode and the RF switch-off has to be strong enough to overcome the effect of the naturally longer sawteeth obtained with NBI heating. A detailed investigation of the here presented sawtooth control technique has not yet been carried-out in JET-ILW H-mode plasmas but promising results with pre-programmed ICRH modulation were obtained in a few cases using moderate NBI power, as discussed next.

In Fig.6 two similar H-mode discharges with constant (left) and modulated (right) ICRH are compared. In both cases the plasma parameters were B_0=2.7T, I_P=2.5MA and ~10MW of NBI power was applied on top of 2-3MW of ICRH power (a). On-axis H minority ICRH at f=42.5MHz (with dipole antenna phasing) was used and the RF power was modulated at 3Hz (duty cycle 75%) in pulse 89976. The typical central densities are comparable to the L-mode discharges discussed earlier, n_{e0}=(5±1)x10^{19}/m^3.
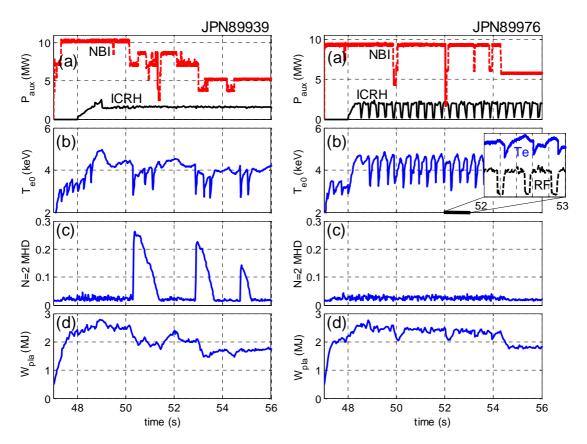

Figure 6: Comparison of two H-mode discharges with constant (89939) and 3Hz modulated (89976) ICRF heating, illustrating the reliable sawtooth pacing and total suppression of the N=2 MHD activity in the latter: (a) NBI and ICRH power; (b) central electron temperature; (c) N=2 MHD mode amplitude; (d) plasma stored energy.

Although the sawtooth dynamics of the non-modulated pulse resembles the L-mode example shown in Fig.2 (89819), the sawteeth are much longer (~1.5s) due to the additional stabilizing effect of the NBI ions and the intensity (and duration) of the N=2 MHD activity is

larger. In some cases, the amplitude of the N=2 mode exceeded the threshold for safe plasma operation and the discharge was stopped by the MHD protection system. When the ICRF power was modulated at 3Hz (right), clear sawtooth pacing was achieved despite the modest ICRH/NBI power fraction (~25%) and the *N*=2 modes were totally suppressed.

Different modulation frequencies have also been tested in H-mode and the results are summarized in Fig.7. The y-axis of the RF=const. case has been extended to 2s to accommodate the very long sawteeth observed. Because higher slowing-down times are expected in H-mode (higher T_e), the duty-cycle of the RF modulation was adjusted for each modulation frequency to allow enough time for the ICRH notch to potentially induce a sawtooth crash: duty-cycle=80% (2.5Hz), 75% (3Hz), 60% (5Hz). In the f_{mod}=2.5Hz case, reliable sawtooth control is achieved but only in the first part of the discharge. At t=52s the NBI power is dropped from 10MW to 5MW and the RF absorption properties are not adequate for sawtooth control in the new conditions. The f_{mod}=3Hz case shows reliable sawtooth pacing throughout the discharge (with constant NBI power) and the sawtooth dynamics is similar to the one obtained in the reciprocal L-mode discharge (Fig.3 - 89821), despite the slightly lower ICRH power and the presence of NBI in the H-mode case. However, unlike the L-mode results, it was not possible to control the sawteeth in the 5Hz RF-modulated discharge. Due to the presence of the stabilizing NBI ions in H-mode, only every second RF notch triggers a sawteeth at the given heating conditions and the effective sawtooth frequency is twice the modulation frequency. During the first ICRH notch during a sawtooth cycle, the removal of RF power does not induce a strong enough perturbation of the core fast ion population to produce a sawtooth crash and the central temperature remains constant (or starts to decrease slowly if the NBI power is not enough to sustain it). When the RF power is re-applied, the central temperature starts increasing again and by the time of the second ICRH notch, the stability conditions are such that the reduction in the fast ion population is sufficient for a sawtooth crash to be induced. There were H-mode examples (with optimized ICRF settings) in which reliable sawtooth control at f_{mod}=5Hz was achieved during short periods (~2s) but a clear validation of sawtooth pacing at high RF modulation frequency throughout the discharge has not yet been achieved.
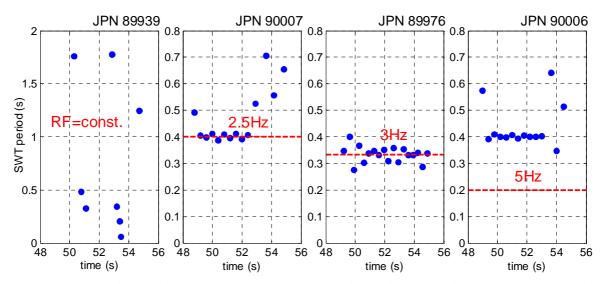

Figure 7: Sawtooth period vs. time for 4 similar H-mode discharges with constant and modulated ICRF power (f_{mod} = 0, 2.5Hz, 3Hz, 5Hz). The duty-cycles were adjusted according to the modulation frequency: 80% (2.5Hz), 75% (3Hz), 60% (5Hz) to allow long enough RF notches. The ICRF heating is not sufficiently optimized for pacing the sawteeth at f_{mod}=5Hz and the effective sawtooth period ends-up being twice the modulation frequency.

The competition between the ICRH power modulation with other stabilizing power sources in the plasma such as NBI and fusion born alpha-particles is a concern for the regular use of this technique in high NBI power discharges and in future fusion reactors. However, the fact that the ICRH power absorption is typically more localized than the ones from NBI and fusion-born alpha particles is encouraging, since the central power densities achieved with ICRH are comparable (if not higher) than the other local power densities even if the ICRH power fraction is modest compared to the other sources.

An example is given in Fig.8, where the ICRH power absorption profile of a standard fundamental H minority ICRH scheme in a D plasma with P_{icrh}=5MW (computed with the full-wave CYRANO code [50]) is compared with the NBI power absorption profile for D ions with P_{nbi}=20MW (computed with the PENCIL code [51]) for typical JET-ILW H-mode conditions: B_0=2.7T, f_{RF}=42.5MHz, n_{e0}=7x10^{19}/m^3, T_e=T_i=6keV, E_{beam}=100keV. An isotropic alpha-particle power source $P_\alpha \propto (n_i T_i)^2$ [52], corresponding to ~10MW of DT fusion power is also included. It is clear from these results that relatively modest fractions of ICRH power can have a dominant influence in the fast ion dynamics in the plasma core due to its localized absorption as compared to NBI and alpha-particle heating. This is consistent with the results shown in section 5, where successful sawtooth pacing was achieved with only 2-3MW of modulated ICRH applied on top of 10MW NBI. The alpha-particle contribution is small in these conditions since the projected fusion power for JET-ILW DT operation (P_{fus}≈10MW) is modest compared to the auxiliary heating. In ITER, where the fusion power is expected to be dominant, the alpha power will be much higher and sufficient amount of ICRH has to be available for potential sawtooth control.

Another encouraging aspect is the fact that, unlike NBI heating (whose associated fast particle distributions depend on the beam injection angle and energy) and alpha-particle sources (which feature isotropic distributions), ICRH absorption acts on specific parts of the fast particle distribution in phase-space, namely injecting perpendicular energy to the minority ions. This feature, associated to the fact that the orbits have to intercept the ion-cyclotron resonance for the particle to absorb the injected RF wave power, leads to an accumulation of particles near the passed-trapped energy boundary, forming the so called 'rabbit ears' in the distribution function of the minority ions [53].
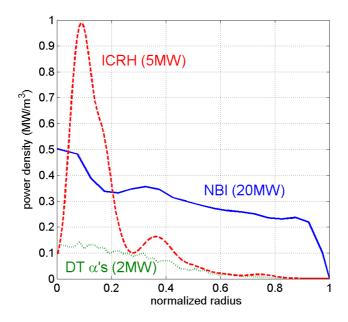

Fig.8: Power absorption profiles for 5MW ICRH (dashed), 20MW NBI (solid) and 2MW DT fusion-born alpha-particles (P_{fus}=10MW, dotted) for typical JET-ILW H-mode conditions.

The exact relationship between the fast ion distribution properties and sawtooth stabilization is not yet fully understood and the optimal parameters (minority concentration, modulation amplitude and frequency, max. absorption position, etc…) for achieving sawtooth control with central ICRH in high power H-modes and DT plasmas in JET-ILW have not yet been identified. Nevertheless, the fact that the ICRH power is more peaked than the ones from the other stabilizing heat sources associated to the high energy / anisotropic fast particle distributions inherent of this heating method makes this technique worth pursuing. Real-time control of the RF modulation (as described in section 4) is likely to be essential in these conditions to assure that the ICRH-induced perturbation in the fast ion distribution is induced at the appropriate time instant during the sawtooth cycle. However, it is clear that in a dominant fusion-power facility with significant alpha-particle power, the ICRH power available has to be significant. 3D Fokker-Planck modelling including orbit effects is necessary to assess the applicability of the described sawtooth control technique in such conditions (as e.g. in ITER DT) but this is outside the scope of the this paper.

6. Time delays (slowing-down)

Although the actual physics of sawtooth stabilisation by fast particles is quite complex and depends on details of the fast particle distribution function in specific regions of the plasma [26-27], the basic characteristics of the described method can be illustrated via first principle plasma parameters such as the slowing down time of the fast particles. This was first studied in [54] in RF switch-off experiments performed at JET. The slowing-down time of the fast ions onto the electrons does not depend on the fast particle energy and is given by $\tau_{SD} = C.\left(k_B T_e\right)^{3/2} / n_e$ [53], where n_e and T_e are the local electron density and temperature, respectively, k_B is the Boltzman's constant and C is a constant that depends on the fast ion mass (protons in this case) and the electron Coulomb logarithm ($\ln \Lambda_e \approx 17$).

Figure 9 shows the time intervals between the RF-off (notch) instants and the respective sawtooth crashes in an L-mode (left) and in an H-mode discharge (right) with the same RF modulation frequency (f_{mod}=3Hz). Both cases were done at B_0=2.7T / I_P=2MA with approximately 4MW of on-axis modulated H minority ICRH at f=42.5MHz (dipole phasing) and P_{NBI}=10MW was applied in the H-mode discharge. The maximum core electron temperatures are respectively T_{e0}=3.5keV (L-mode) and T_{e0}=4.5keV (H-mode), and the central plasma density is similar in the two cases, n_{e0}=5x10^{19}/m^3. The dotted traces represent the electron slowing-down time τ_{SD} computed from the experimental n_{e0} and T_{e0} signals. The fluctuation in these traces is due to the variation of the central electron temperature during the sawtooth cycles.
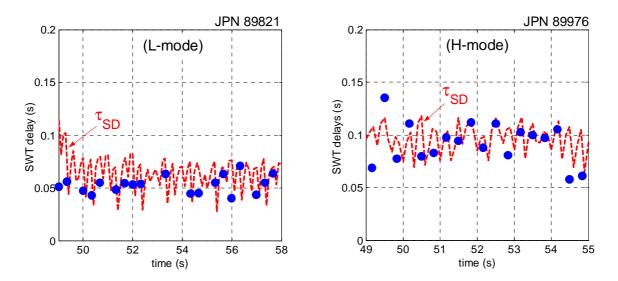
Figure 9: Time delays between the RF switch-off instants and the sawtooth crashes for an L-mode (left) and an H-mode (right) discharge as function of time. P_{icrf}=4MW of central ICRH modulated at 3Hz was applied in both cases. The dashed curves represent the electron slowing-down time τ_{SD} inferred from the core n_e and T_e measurements.

As expected from first order RF theory, the time delays between the RF switch-off instants and the sawtooth crashes are comparable to the electron slowing down time in both cases. In L-mode the agreement is better since ICRF heating is the dominant mechanism influencing sawteeth stabilization. Although the agreement is also good in the H-mode example shown, there is evidence of sawtooth pacing with longer sawtooth delays than the electron slowing-down time in some pulses (as for #89976 at t=49.5s). This suggests that the additional stabilization character of the NBI ions can influence (or delay) the RF-induced sawtooth triggering, but more studies are needed to quantify this effect.

The correlation between the slowing-down dynamics of the RF accelerated ions and the sawteeth triggering times is further illustrated in Fig.10, where the results of a statistical analysis of a number of L-mode (left) and H-mode (right) discharges are shown. The curves represent the experimental distribution function of the waiting time from the start of the ICRH notch to the next sawtooth crash. This distribution time represent the relative number of triggering events detected in a narrow time window as function of the time delay between the ICRH power notches and the subsequent sawtooth crashes. The data are taken from a series of similar discharges (with different RF modulation frequencies). The statistical results confirm that the highest sawtooth triggering probability is indeed centred around the lower boundary of the typical electron slowing-down time of the fast ions, both for the L-mode (40-70ms) as for the H-mode case (80-110ms). The fact that the probability distribution is broader in the latter corroborates the fact that it is more difficult to lock the sawtooth cycle to the RF modulation frequency when the stabilizing effect of the fast NBI ions is present and that other process contribute to the impact the of the fast ion distribution function on the sawtooth stabilisation in these conditions.
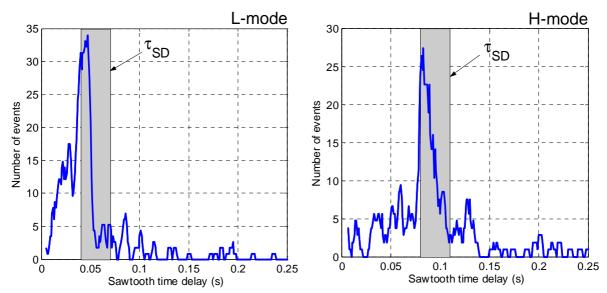
Figure 10: Statistical analysis of the delays between the RF switch-off time and the sawtooth crashes for L-mode (left) and H-mode (right) plasmas. The grey areas represent the typical electron slowing-down time of the fast ions in each case.

In H-mode discharges, it was generally observed that when the sawtooth delays exceed ~$1.5\tau_{SD}$, the sawtooth pacing is not efficient and only every other sawtooth is triggered by the RF modulation (similar to Fig7, #90006). One additional effect that contributes to the sawtooth dynamics in H-mode is the 2nd harmonic ICRH absorption of the NBI ions [53]. The RF-accelerated NBI ions achieve high energies and mostly slow down on the electrons and therefore also contribute to the sawtooth pacing process. This effect may, to some extent, compensate for the background stabilizing character of the NBI ions and explain why the sawtooth delays are still well correlated with the slowing-down time in most of the H-mode discharges studied.

The statistical analysis of the time lags, even if good as a first approximation, is not necessarily conclusive, since it can be potentially affected by spurious effects such as accidental coincidences or particular features of the experimental signals. Therefore two complementary and more advanced techniques have also been deployed to consolidate the determination of the correlation between the switching-off of the ICRH and the triggering of sawteeth: Transfer Entropy and Recurrence Plots. Transfer Entropy is an information theoretic criterion, which was originally developed to determine the causal relations between time series [55]. It can be used to determine the time of maximum influence between signals and in this sense it has already been applied to the assessment of the efficiency of ELM triggering by pellets [56]. Recurrence plots constitute a quite consolidated tool for the analysis of the dynamical properties of systems [57]. The version called Joint Recurrence Plots has been devised to investigate the mutual influence between dynamical systems. This approach has also been very useful in the determination of the effectiveness of the pellets in triggering ELMs [58]. On important point to appreciate is that both Transfer Entropy and Recurrence Plots do not consider only the time lags between signals but take into account the behaviour of the entire time series and can therefore provide more reliable indications. With regard to the experiments of sawtooth triggering with ICRF modulation reported here, the two methods have been use to analyse the same discharges shown on Fig. 10. The results of both methods confirm the conclusions derived by the direct analysis of the time lags between the notches of the RF and the respective time crashes: in both L and H mode plasmas these intervals are consistent with the lower bund of the slowing down time of the fast ions on the electrons.

7. Summary

Reliable sawteeth control was achieved with modulated on-axis ICRF heating in JET-ILW L-mode discharges with B_0=2.7T, I_P=2MA. Central H minority ICRH at f=42.5MHz (dipole phasing) with P_{icrh}=3-4MW was used with modulation frequencies ranging from 2-5Hz. While the non-modulated reference plasmas were characterized by long sawteeth (τ>0.5s) and considerable N=2 MHD activity following the sawtooth crashes, the discharges in which the sawteeth were paced with $f_{mod} \geq$3Hz showed complete suppression of the N=2 modes. The triggering efficiency (number of RF-triggered sawteeth over number of RF notches) is typically above 80% in all cases studied. The lag time between the RF switch-off instant and the sawtooth crash is correlated to the electron slowing-down time of the fast ions and does not depend on the RF modulation frequency in the studied range.

A real time control network was developed to control the RF power waveform according to the sawtooth dynamics detected in real time during the discharge. This has the advantage of avoiding unnecessary RF-notches and minimizing the RF switch-off time, since the power is re-applied immediately after a sawtooth crash is detected. With real-time control, the triggering efficiency is practically 100% and the equivalent duty cycle of the RF modulation is increased as compared to pre-programmed RF modulation.

Preliminary investigations indicate that this technique can also be applied to moderate NBI power H-modes (B_0=2.7T, I_P=2MA, P_{NBI}~10MW) at moderate ICRH power levels (2-4MW), despite the stabilizing contribution of the NBI ions. In this case, reliable sawtooth pacing requires more careful tuning of the ICRF heating parameters (RF power, H conc.) according to the discharge properties, but once the optimal conditions are reached, the triggering efficiency is comparable to L-mode ($\geq$80%). Sawtooth control at high modulation frequencies (5Hz) is harder to achieve than in L-mode due to the stabilizing effect of the background NBI ions. The delays between the RF switch-off instants and the sawtooth crashes also correlate to the electron slowing-down time of the fast ions in most cases, but there are indications that other effects – such as the NBI stabilization – contribute to the actual time delay for a sawtooth to be triggered but more in-depth studies are needed to quantitatively assess this effect. Using real-time control of the RF-modulation frequency in these conditions is expected to increase the reliability of sawteeth control in H-mode and is planned for future experiments.

Further experimental studies are necessary to determine the best settings for sawtooth pacing in high power H-modes and which range of modulation frequencies can be used to eventually validate this technique as a standard tool for scenario development. One important question is whether pacing the sawteeth at an optimal frequency is beneficial for minimizing high-Z core impurity accumulation (often observed in high power JET-ILW H-modes) and how it compares with the impurity screening obtained by applying constant RF power on-axis (and not controlling the sawteeth). Another important question is whether this technique can also be used in DT fusion plasmas, where the α-particles (in addition to the NBI ions) also contribute to the background sawteeth stabilization. This can be partly assessed in JET by operating at high NBI power, but numerical tools that properly describe the competition between the different fast ion sources taking into account their different particle distributions and the synergy between them is still under development.

References

[1] M.D. Kruskal and Oberman C.R. 1958 *Phys. Fluids* **1** 275
[2] M.N. Bussac et al., 1975 *Phys. Rev. Lett.* **35** 1638
[3] H.D. Hazeltine et al., Phys. Fluids **18**, 1778 (1975)
[4] S. von Goeler et al., Phys. Rev. Lett., vol. 33, 1974, pp 1201
[5] J. P. Graves *et al* 2015 *Plasma Phys. Control. Fusion* **57** 014033
[6] I. Chapman et al 2010 Nucl. Fusion 50 102001
[7] O. Sauter *et al.*, Phys. Rev. Lett. **88**, 105001 (2002).
[8] I. T Chapman *et al.*, Nucl. Fusion **50**, 102001 (2010).
[9] C. Angioni at al., 2003 *Nucl. Fusion* **43** 455
[10] A. Mück *et al* 2005 *Plasma Phys. Control. Fusion* **47** 1633
[11] M. Lennholm et al., Phys. Rev. Lett., vol. 102, 2009, 115004
[12] M. Lennholm et al., Fusion Sci. Technol., vol. 55, 2009, pp. 45-55
[13] J.I. Paley et al., Plasma Phys. Control. Fusion, vol. 51, 2009 , 055010
[14] G. Witvoet et al., Nucl. Fusion, vol. 51, 2011, 073024
[15] G. Witvoet et al., Nucl. Fusion, vol. 52, 2012, 074005
[16] T.P.Goodman et al., Phys. Rev. Lett., vol. 106, 2011, 245002
[17] M. Lauret et al., Nucl.Fusion, vol. 52, 2012, 062002
[18] S. Nowak et al., Nucl. Fusion, vol. 54, 2014, 033003
[19] G. Witvoet *et al* 2011 *Nucl. Fusion* **51** 103043
[20] R.B. White et al., *Phys. Rev. Lett.* **60** 2038
[21] R.B. White et al., 1989 *Phys. Rev. Lett.* **62** 539
[22] R.B. White et al., 1990 *Phys. Fluids* B **2** 745
[23] Coppi B. Et al., 1989 *Phys. Rev. Lett.* **63** 2733
[24] F. Porcelli et al., 1991 *Plasma Phys. Control. Fusion* **33** 1601
[25] F. Porcelli et al., Plasma Phys. Controlled Fusion, vol. 38, 1996, 2163
[26] J.P. Graves et al., Phys. Rev. Lett. vol. 102, 2009, 065005
[27] J.P. Graves et al., 2012 *Nat. Commun.* **3** 624
[28] J.P. Graves *et al* 2010 *Nucl. Fusion* **50** 052002
[29] J.P. Graves et al., Fusion Sci. Technol., vol. 59, 2011, pp. 539-548
[30] I.T. Chapman et al., Plasma Phys. Controlled Fusion , vol. 53, 2011, 013001.
[31] I.T. Chapman *et al* 2012 *Nucl. Fusion* **52** 063006
[32] M. Lennholm et al., Nucl. Fusion, vol. 51, 2011, 073032
[33] L.-G. Eriksson *et al* 2004 *Phys. Rev. Lett.* **92** 235004
[34] L.-G. Eriksson *et al* 2006 *Nucl. Fusion* **46** S951
[35] F. Romanelli and JET EFDA Contributors 2013 *Nucl. Fusion* **53** 104002
[36] G.F. Matthews *et al* 2011 *Phys. Scr.* **T145** 014001
[37] R. Neu *et al* 2013 *Phys. Plasmas* **20** 056111
[38] G.F. Matthews *et al* 2013 *J. Nucl. Mater.* **438** S2–10
[39] E. Lerche et al., *Nucl. Fusion* **56** (2016) 036022
[40] M. Goniche *et al.*, Proc. 41st EPS Conference on Plasma Physics, O4.129, Berlin (2014)
[41] E. Joffrin *et al* 2014 *Nuclear Fusion* **54** 013011
[42] M.N.A. Beurskens *et al* 2013 *Plasma Phys. Control. Fusion* **55** 124043
[43] R. Neu *et al.*, *Plasma Phys. Control. Fusion* **49** 12B (2007) B59-B70
[44] T. Pütterich *et al* 2013 *Plasma Phys. Control. Fusion* **55** 124036

[45] R. Dux *et al* 2009 *JNM* **390–391** 858

[46] M. Lauret et al., accepted for publication in Plasma Physics and Controlled Fusion, 2016.

[47] M. Lennholm et al., Nucl. Fusion, vol. 56, 2016, 016008.

[48] M. Lennholm, "*Real Time Control of the Sawtooth Instability in Fusion Plasmas with Large Fast Ion Populations*", PhD Thesis, 2014, University of Eindhoven, The Netherlands

[49] E. Lerche *et al*, AIP Conf. Proc. 1187 p.93 (2009)

[50] Ph. Lamalle, "*Non-local theoretical generalization and tri-dimensional numerical study of the coupling of an ICRH antenna to a tokamak plasma*", PhD Thesis, 1994, University of Mons, Belgium,

[51] C. Challis *et al.*, Nucl. Fusion **29** (1989), p.563.

[52] Palpha~n2T2

[53] T.H. Stix, "Waves in Plasmas" (1992) AIP, New York

[54] D. J. Campbell *et al*., Proc. 15th EPS Conference on Controlled Fusion and Plasma Heating, Dubrovnik (1988)

[55] T.Schreiber, Phys. Rev. Lett. **85**, 461 (2000).

[56] A.Murari et al Nucl. Fusion **56** (2016) 026006 (11pp)

[57] N.Marwan wt al Physics Reports **438** (2007) 237 – 329)

[58] A.Murari et al Nucl. Fusion **56** (2016) 076008 (12pp)